www.czasopisma.pan.pl PAN POLSKA AKADEMIA NAUK www.journals.pan.pl

Arch. Min. Sci. **69** (2024), 2, 289-302

Electronic version (in color) of this paper is available: http://mining.archives.pl

DOI: https://doi.org/10.24425/ams.2024.150346

RENYUAN WU[1,2], SHUANGLI WANG[3*], CHENGJUN WANG[1,2]

THE INFLUENCE OF ROPE GUIDE SLEEVE CLEARANCE ON THE LATERAL OSCILLATION OF ROPE GUIDED CONVEYANCE IN MINE HOIST SYSTEM CAUSED BY THE AERODYNAMIC FORCE

The lateral oscillation behaviour of rope guided conveyances was so complicated that the rope guided hoisting system hasn't been understood thoroughly so far. In this study, the CFD tool was used to obtain the aerodynamic force acting on the conveyance by writing a user-defined function (UDF), and then the oscillation behaviour of rope guided conveyances was investigated numerically by Matlab with the variation clearance between the guide sleeve and the guide rope. A non-smooth oscillation model of the rope guided conveyance was established by considering the clearance between the guide sleeve and the guide rope. Results show that the aerodynamic buffeting forces had a notable influence on the oscillation behaviour of rope guided conveyances during the conveyances passing each other. The lateral acceleration of the rope guided conveyances showed a minor change with the increase of the clearance. However, the oscillation amplitude of the conveyances manifested a positive correlation with the rope guide sleeve clearance.

Keywords: rope guided hoisting system; aerodynamic buffeting force; rope guided conveyance; lateral oscillation; rope guide sleeve clearance

1. Introduction

Hoisting systems are of significant importance in the underground mining industry, which is used to transport and handle ore, waste, materials, types of equipment and personnel. Compared to a fixed guide hoisting system, a rope guide hoisting system has some advantages, such as less

[1] ANHUI UNIVERSITY OF SCIENCE AND TECHNOLOGY, MECHANICAL INDUSTRY KEY LABORATORY OF INTELLIGENT MINING AND BENEFICIATION EQUIPMENT, CHINA
[2] ANHUI UNIVERSITY OF SCIENCE AND TECHNOLOGY, SCHOOL OF ARTIFICIAL INTELLIGENCE, CHINA
[3] ANHUI UNIVERSITY OF SCIENCE AND TECHNOLOGY, JOINT NATIONAL-LOCAL ENGINEERING RESEARCH CENTRE FOR SAFE AND PRECISE COAL MINING, CHINA

* Corresponding author: wsly0669@foxmail.com

resistance to ventilation air flows, shorter installation times, lower capital costs and reduced maintenance requirements [1-3]. However, affected by the mine ventilation, tension and conveyance loading quality, etc., the lateral oscillation behaviour of rope guided conveyances is so complex that the rope guided hoisting system hasn't been understood thoroughly [4-6]. There are few systematic research reports, and the rope guided hoisting system is lacking a complete design guideline [7].

By using the onboard strap-down inertial navigation system (INS), Buchinski [8] recorded skip position and attitude successfully, but the calibration of another inertial measuring system showed drift outside the performance specification [9]. Fixed lasers measuring the distance between the conveyance and the shaft sidewall is another technique, but the random roughness and unstraightness of the shaft sidewall might affect the measurement precision [10].

With the development of computational fluid dynamics (CFD), CFD has been a powerful tool to study problems in the rope guided shaft hoisting system [11-13]. In order to investigate the distribution of air pressure when the rope guided conveyance is running in the shaft and obtain the lateral aerodynamic force, Xu Changlei [11] simulated the rope guided conveyance running in the shaft and the variation of air flow field by the code Fluent. Quan Situ etc. [12] investigated the influence of guide ropes, air pressure and Coriolis effect on the motion of rope guided skips in the production shaft with the software of SolidWorks CosmosFlow and ANSYS WorkBench, predicting the skip velocity could be increased to 4000 fpm. The steady-state aerodynamic force and transient aerodynamic forces acting on the rope guided conveyance were computed based on skip hoisting simulation with Star-CD [13]. With the UDFs of rope guide conveyances motion loaded by Fluent, it was found that the behaviours of rope guided conveyances were greatly affected by the ventilation air speed and shaft layouts [5,14].

The rope-guided conveyance should be equipped with guide sleeves, and the clearance exists between the guide sleeve and the guide rope. With the conveyance hoisted up and down, the clearance between the guide sleeve and the guide rope increases continuously due to the wear and tear between the guide sleeve and the guide rope [15]. Therefore, the consideration of the clearance between the guide sleeve and the guide rope is essential for establishing the motion equations of rope guided conveyances. In this study, the CFD tools were used to obtain the aerodynamic force acting on the conveyance, and then the behaviour of rope guided conveyances was investigated numerically with different clearances between the guide sleeve and the guide rope.

2. Numerical models

2.1. Mathematical models

A detailed description of the fluid-structure interaction (FSI) technique applied to simulate the lateral oscillations of rope guided conveyances has been presented in our previous article [16].

The rope guided hoisting system was mainly composed of a hoist winder, hoisting rope, conveyance 1, conveyance 2, guide ropes, guide sleeve, balance rope and tensioning weight, as shown in Fig. 1 [17]. The hoist winder drove the conveyance moving up and down in the shaft by frictional force occurring between the hoist winder and the hoisting rope. The conveyance was equipped with guide sleeves to travel along the guide ropes. The guide rope through the guide sleeve was tensioned by the tensioning weight to orient the motion of the conveyance.

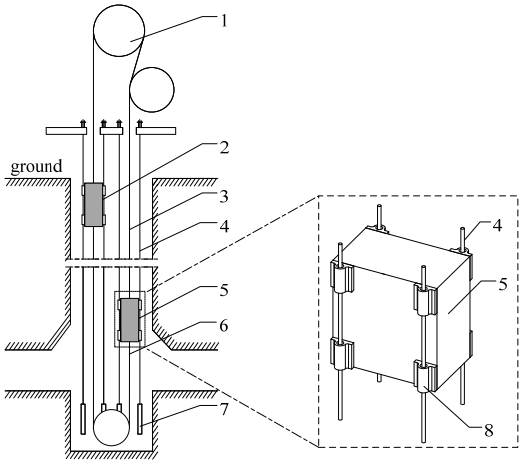

1 – winder; 2 – conveyance 1; 3 – hoist ropes; 4 – guide ropes; 5 – conveyance 2; 6 – balance ropes; 7 – tension weight; 8 – guide sleeve

Fig. 1. Schematic diagram of tower mounted Koepe winders rope guided hoisting system

As illustrated in Fig. 2, there existed a clearance between the guide sleeve and the guide rope attributed to the radius difference. Since the conveyances were hoisted up and down alternately, the guide sleeve was constantly worn by the guide rope. Moreover, the clearance between the guide sleeve and the guide rope increased with wear and tear between them, which contributed to the lateral oscillation property change of the rope guided conveyance.

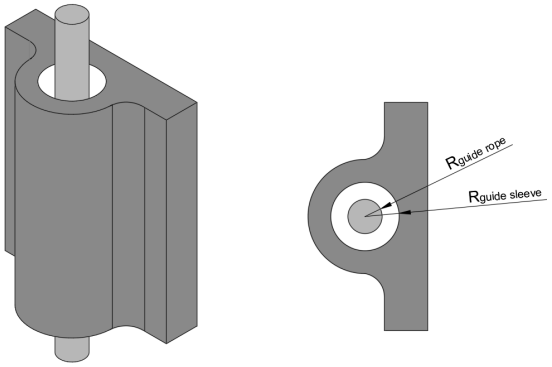

Fig. 2. Schematic diagram of the clearance between the guide sleeve and the guide rope

In order to balance the weight of the hoisting rope on both sides of the winder during the hoisting process, the friction hoisting system was usually equipped with balance ropes. Since the guide ropes, the hoisting ropes, and the balance ropes had a long length in the mine hoisting system, the rope mass was relatively large. The mass of the wire rope itself should not be ignored in studying the oscillation behaviour of rope guided conveyance, otherwise, mistakes

might occur in the calculation of the lateral displacement. According to the Rayleigh method [18], the equivalent mass was calculated by adding up the conveyance mass and one-third of the total mass of the guide ropes, hoisting ropes and balance ropes.

As shown in Fig. 3, the Oxyz coordinate system was first established in the rope guided shaft. Then, the dynamic mathematical model was established by removing the constraint of the guide rope on the conveyance and replacing it with the constraint force based on the Oxyz coordinate system. Due to the existence of the clearance, the lateral vibration model of the rope guided conveyance hoisting system was transformed from a smooth model into a non-smooth model. The conveyance was treated as the dynamic analysis object of the non-smooth mathematical model. Furthermore, the lateral force acting on the conveyance mainly included the lateral aerodynamic force during the hoisting and lowering of the conveyance, the east-west Coriolis force caused by the earth's rotation, and the elastic restoring force of the rope guided hoisting system.

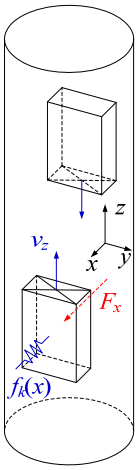

Fig. 3. Dynamic mathematical model of rope guided shaft hoisting system

The rotation phenomenon of the hoisting conveyance around the x-axis, y-axis and z-axis displayed slightly in terms of the actual measurement of multi-rope hoisting mines [8], and the lateral swing amplitude of the hoisting conveyance in the horizontal y-axis direction was much smaller than that in the horizontal *x*-axis direction. Herein, without considering rotation angles and the lateral swing amplitude in the horizontal *y*-axis direction, the differential equation of the non-smooth lateral vibration of the hoisting conveyance along the horizontal *x*-axis based on vibration mechanics presented as:

$$\left(m+m_{eq}\right)\frac{\mathrm{d}^2x}{\mathrm{d}t^2}=F_x-f_k\left(x\right) \tag{1}$$

Where, m was the total mass of the hoisting conveyance including the load; m_{eq} was the sum of the equivalent mass of the guide rope and the hoisting wire rope; x was the displacement of the hoisting conveyance in the x direction; F_x was the disturbance force of the hoisting conveyance in the x direction.

Since the length of the rope guide rails and hoisting ropes used in the mine hoisting system was manifested as long as several hundred metres and the mass of the ropes was relatively larger compared to the terminal mass of the conveyance, the influence of the rope mass on the lateral vibration of the hoisting conveyance should be taken into consideration. The Rayleigh method [18] was applied to calculate the transverse equivalent mass of the wire rope, as shown below. The guide rope had no effect on the hoisting conveyance on the condition that the displacement of the conveyance in the x direction was less than the gap between the guide sleeve and the guide rope, so the equivalent mass did not include the guide rope part. However, the gap between the guide sleeve and the guide rope might have a noticeable effect on the motion of the hoisting conveyance in the case that the displacement of the conveyance in the x direction was greater than the distance between the guide sleeve and the guide rope, the guide rope part should be taken into account in the calculation of the equivalent quality. The equivalent mass m_{eq} of the guide rope and the hoisting wire rope could be obtained by the Rayleigh method as:

$$m_{eq} = \begin{cases} n_H \dfrac{q_h l_h}{3} + n_T \dfrac{q_t l_t}{3} + n_R \dfrac{q_r l_r}{3}, & x < -e \\ n_H \dfrac{q_h l_h}{3} + n_T \dfrac{q_t l_t}{3}, & -e < x < e \\ n_H \dfrac{q_h l_h}{3} + n_T \dfrac{q_t l_t}{3} + n_R \dfrac{q_r l_r}{3}, & x > e \end{cases} \tag{2}$$

Where, n_H was the number of hoisting ropes; q_h was the linear density of the hoisting rope; l_h was the length of the hoisting rope on the conveyance side; n_T was the number of tail ropes; q_t was the linear density of the tail rope; l_t was the length of the tail rope on the conveyance side; n_R was the number of guide ropes at the conveyance; q_r was the linear density of the guide rope; l_r was the length of the guide rope; e was the gap between the guide sleeve and the guide rope.

The elastic restoring force $f_k(x)$ of the rope guided hoisting system could be presented as:

$$f_k(x) = \begin{cases} n_H k_H x + n_T k_T x + n_R k_R (x + e), & x < -e \\ n_H k_H x + n_T k_T x, & -e < x < e \\ n_H k_H x + n_T k_T x + n_R k_R (x - e), & x > e \end{cases} \tag{3}$$

Where, k_H was the lateral equivalent spring stiffness of the hoisting rope at the conveyance; k_T was the lateral equivalent spring stiffness of the tail rope at the conveyance; k_R was the lateral equivalent spring stiffness of the rope guide rail at the conveyance.

The Coriolis force exerted on the moving conveyance was caused by the earth's rotation. The conveyance was vectored by eastward Coriolis force when hoisted up. Additionally, the Coriolis force on the conveyance was westward when the conveyance was lowered down. Therefore, the disturbance force in the east-west direction contained the Coriolis force and the aerodynamic force, while the disturbance force in the north-south direction did not contain the Coriolis force. If the conveyance was not arranged north-south (or east-west), the Coriolis force needed to be decomposed. The aerodynamic force was obtained by numerically solving the fluid governing

equations of computational fluid dynamics, while the Coriolis force could be calculated by the formula as follows [9]:

$$F_C = 2mv_z\omega\cos\phi \tag{4}$$

Where, m was the mass of the hoisting conveyance, including the self-weight and load of the conveyance; v_z was the longitudinal hoisting speed of the hoisting conveyance; ω was the angular velocity of the earth's rotation; ϕ was the latitude of the mine.

2.2. Shaft parameters

It could be known from the empirical formula of aerodynamics that the aerodynamic force was proportional to the square of the relative velocity of the gas, and thus, the hoisting speed manifested a direct correlation with the aerodynamic force acting on the hoisting conveyance. The swing of the conveyance was investigated in this section with the operation condition that the hoisting speed of the conveyance was set as 8 m/s, the ventilation speed of the shaft was taken as 2 m/s, and the running direction was downward. The shaft layout used in this section is shown in Fig. 4, and the variation of the velocity with time is displayed in Fig. 5.

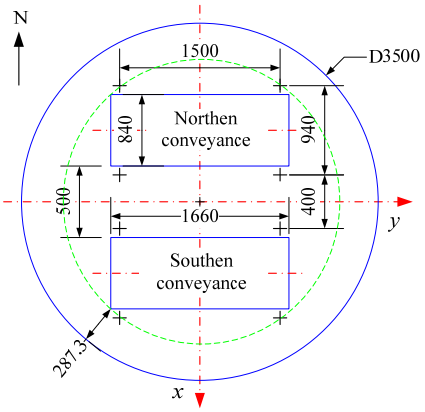

Fig. 4. The shaft layout of mine conveyances

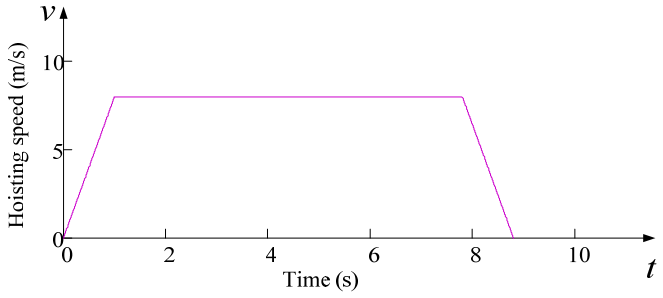

Fig. 5. Time-speed diagram in vertical direction

The rope guides were equipped with sealed steel wire ropes and the bottom weight tensioning system. The length of the rope guide was 75 m, and the hoisting distance was 62.4 m. TABLE 1 shows the main shaft parameters.

TABLE 1

The main shaft parameters

Hoist ropes	4 off, 13 mm, 0.586 kg/m
Tail ropes	1 off, 26 mm, 2.33 kg/m
Guide ropes	4 off per conveyance, 24 mm, 3.22 kg/m
Conveyance mass	1.6 t
Hoisting distance	62.4 m
Hoisting speed	8 m/s
Payload	1.0 t
Method of tensioning	Weight
Tension load	1000 kg per guide rope
Ventilation direction	2 m/s, downcast

2.3. CFD modelling

The PISO algorithm of ANSYS Fluent 15.0 was used as the solving algorithm in the simulation. The upper entrance was set as the pressure inlet boundary condition, the bottom shaft was set as the pressure outlet boundary condition, and the other boundaries were set as the no-slip wall. The hoisting speed of the conveyance and the aerodynamic force calculated for the conveyance were defined by writing a user-defined function (UDF) and then outputted to a text file. The longitudinal motion of the hoisting conveyance was achieved by spring smoothing methods and local cell remeshing methods in the ANSYS Fluent software. Since the local element meshing method could only be applied to tetrahedral meshes, the fluid computational domain of the rope guide mine hoisting system was divided into tetrahedral meshes, as exhibited in Fig. 6.

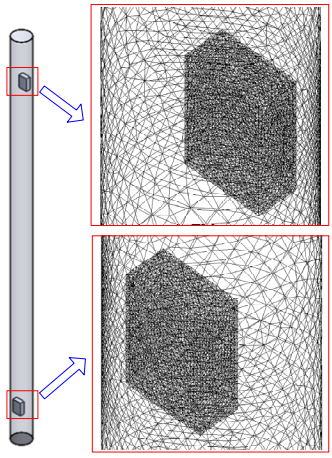

Fig. 6. Meshes used for CFD calculates

The movements of conveyance have been implemented using a dynamic mesh with the local cell remeshing method in ANSYS Fluent. The fluid computational domain was constituted with about 4×105 control volumes. Since the Reynolds number of the air flow in the shaft was much larger than 2300 when the conveyance was lifted up and down, the air flow in the shaft was manifested as turbulence [19]. In this paper, the Shear stress transport SST k-ω turbulence model was used to simulate the air flow during the conveyance hoisted up and down in the shaft. The hoisting speed was 8 m/s, and the time of the conveyance running was 8.8 s. The time step was set as 0.001 s, the calculated steps were 8800 steps and the maximum number of iterations per step was set to 200.

3. Results and discussion

When the hoisting conveyances pass each other, the distributions of the air pressure and air velocity around the conveyances significantly change, attributing to the room variation in the shaft, which might contribute to the lateral oscillation of the conveyances.

As exhibited in Fig. 7, air pressure was maximised at the top of the lift-up conveyance compared with the pressure in other regions due to the downward ventilation direction. The maximal pressure of the descending conveyance occurred at the bottom region during the running process. The minimum value of air pressure appeared around the edges of the top of the lift-up conveyance. The pressure around the hoisting conveyances reduced as they approached each

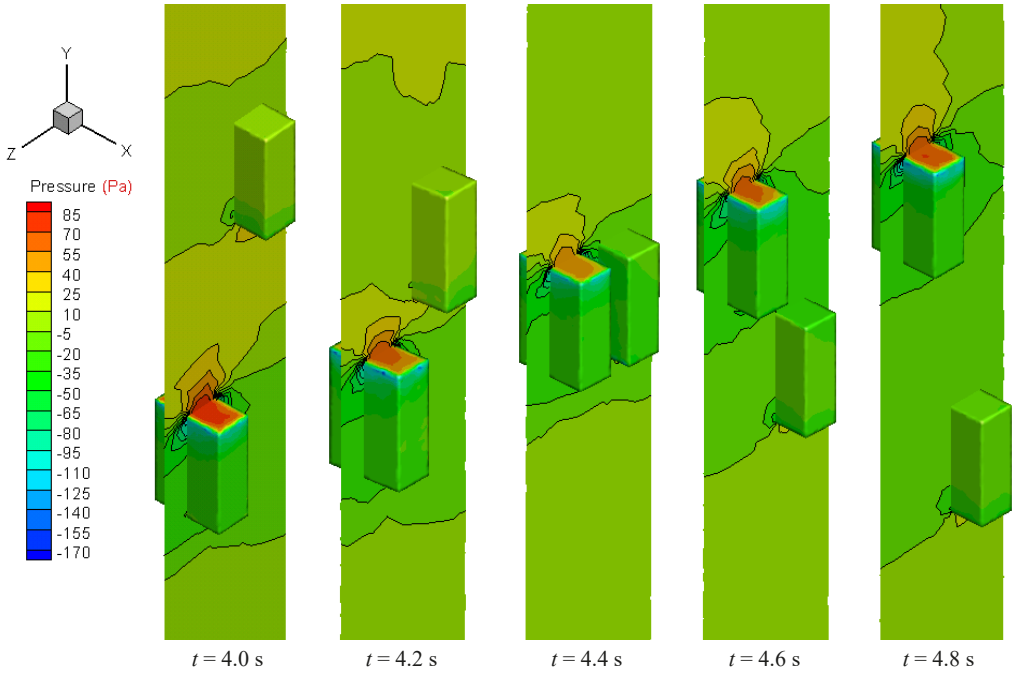

Fig. 7. Pressure contours of the conveyances and the symmetry plane in the middle of the shaft during the two conveyances passing each other

other between times 4.0 s and 4.4 s. Moreover, the pressure around the conveyances increased with the two hoisting conveyances being separated from time 4.4 s to 4.8 s.

As displayed in Fig. 8, two vortexes appeared around the ascending conveyance, which might have contributed to the negative pressure near the conveyance wall. The vortex approaching the lowering conveyance was diminished during the conveyances coming to each other. The increase of air flow velocity might be attributed to the reduction of the pressure between the conveyances during the meeting process. One vortex near the inside wall of the descending conveyance occurred with the conveyances separated due to the variation of the pressure near the lowering conveyance.

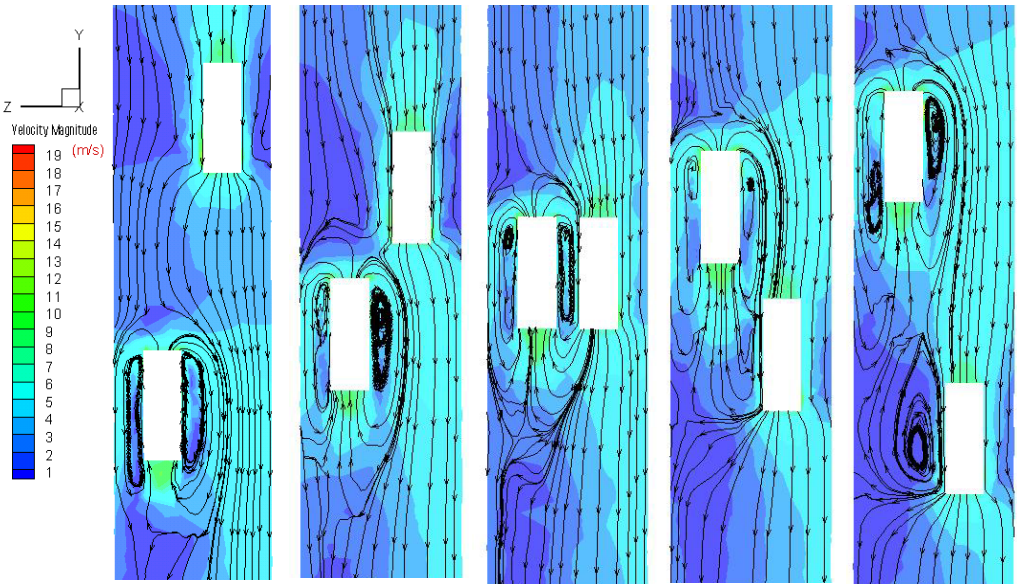

(a) $t = 4.0$ s (b) $t = 4.2$ s (c) $t = 4.4$ s (d) $t = 4.6$ s (e) $t = 4.8$ s

Fig. 8 Velocity contour and streamlines on the plane $x = 0$

Parallel User-defined functions were written to calculate and output the lateral aerodynamic forces acting on the conveyances. The non-smooth lateral vibration model was solved numerically using Matlab. The lateral oscillation characteristics of the conveyances were calculated when the clearance between the guide sleeve and the rope guide was 0, 2 mm, 4 mm, 6 mm and 8 mm, respectively. As shown in Fig. 9 and Fig. 10, the acceleration changed little with the variation of the clearance during the conveyances running up and down. However, the amplitudes of the velocity and displacement increased obviously with the clearance between the guide sleeve and the rope guide.

Since the shaft was ventilated downward, the lateral aerodynamic force of the hoisting conveyance was proportional to the square of the sum of the hoisting speed and the ventilation speed. The lateral aerodynamic force of the descending conveyance was proportional to the square of the difference between the lowering speed and the ventilation speed. As exhibited in Fig. 9(a) and Fig. 10(a), the amplitude of the lateral aerodynamic force of the ascending southern conveyance reached a higher level than that of the descending northern conveyance

before the conveyance passed each other. However, the value of the lateral aerodynamic force showed an opposite tendency during the meeting process. Moreover, the lateral aerodynamic force of the ascending and descending conveyance ranged from –27.0930 N to 45.9497 N and from –84.6015 N to –83.5776 N, respectively.

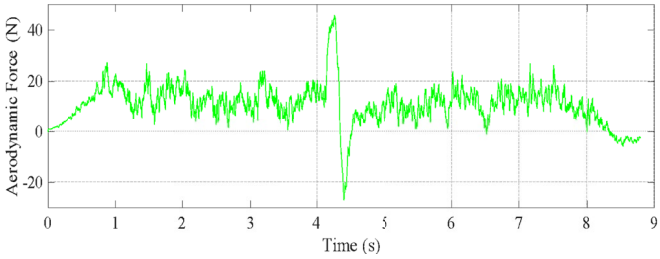

(a) The lateral aerodynamic force

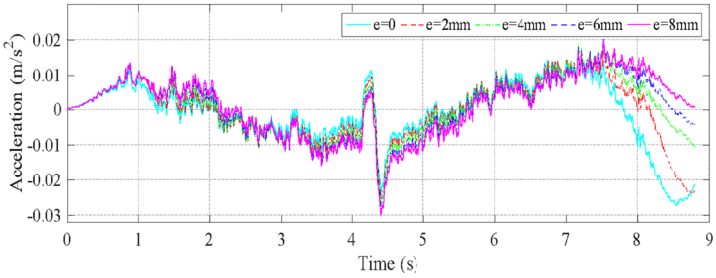

(b) The lateral acceleration

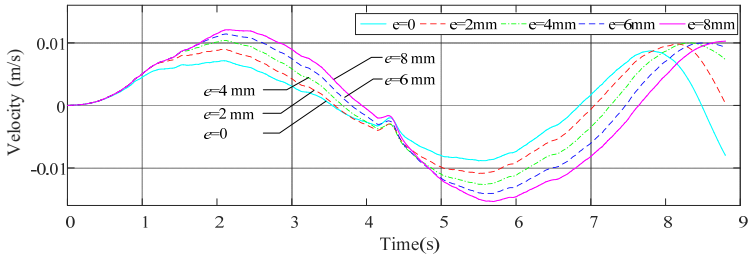

(c) The lateral velocity

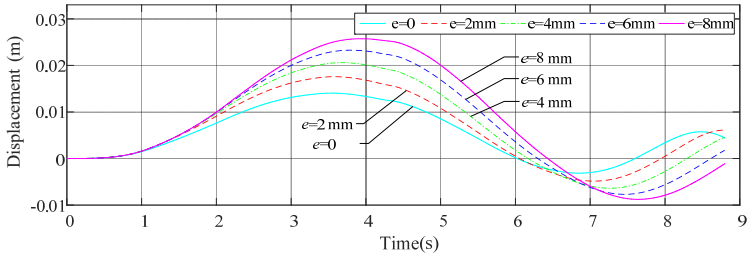

(d) The lateral displacement

Fig. 9. Simulation results of ascending conveyances in *x* direction

The lateral aerodynamic force acting on the southern conveyance was directed to the south, a positive orientation referencing the setting coordinate system during the conveyance passing each other, and the lateral aerodynamic force received by the northern conveyance was directed to the negative orientation. As exhibited in Fig. 9(d) and Fig. 10(d), the oscillation amplitude of

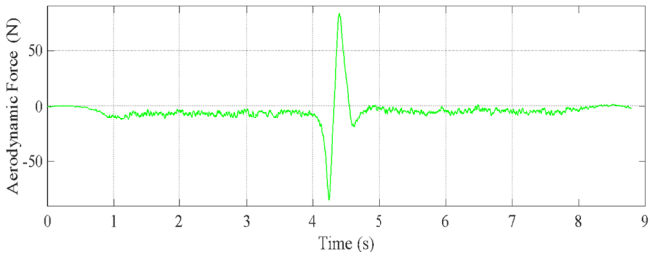

(a) The lateral aerodynamic force

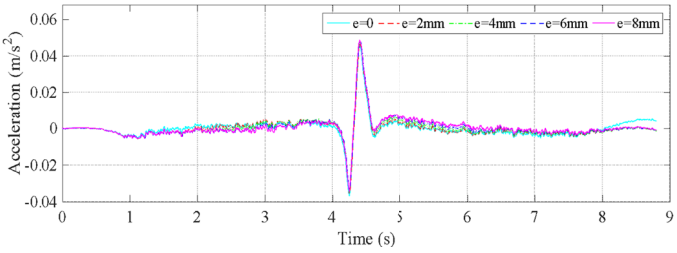

(b) The lateral acceleration

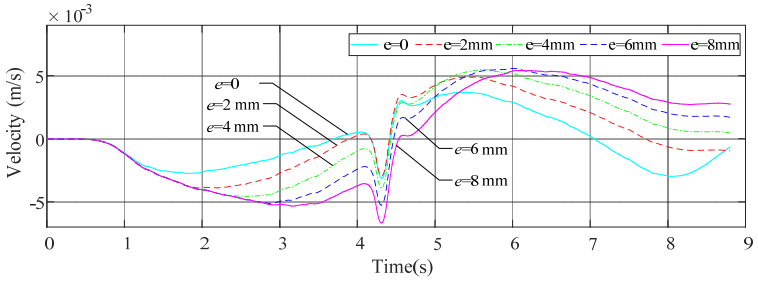

(c) The lateral velocity

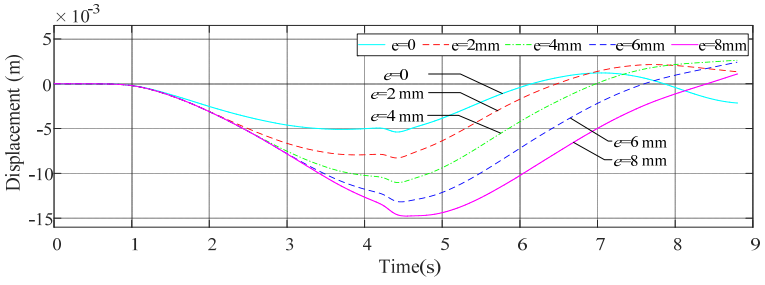

(d) The lateral displacement

Fig. 10. Simulation results of descending conveyances in *x* direction

the southern conveyance in the positive direction manifested a much larger value than that in the negative direction during the hoisting process, while the displacement amplitude of the northern conveyance showed a reverse trend to the southern conveyance during the lowering process.

It could be seen from Fig. 9(d) and Fig. 10(d) that the lateral oscillation period of the conveyance manifested longer with the increase of the clearance between the guide sleeve and the guide rope. Furthermore, the time of maximum positive displacement of lift-up conveyance changed from time 3.5 s with a clearance 0 to time 3.95 s with a clearance 8 mm. Moreover, the maximum displacement occurred at the moment that the lateral velocity of the lift-up conveyance changed from a positive value to zero. As exhibited in Fig. 9(d), the occurrence of the negative maximum displacement of the lowering conveyance changed from time 4.4 s with clearance 0 to time 4.5 s with clearance 8 mm.

As shown in Fig. 10(c), the lateral velocity of the lowering conveyance increased from a negative value to approximate zero at about time 3.7 s to time 4.3 s with the variation of the clearance before the conveyance meeting. However, the other rapid reversal of lateral velocity in tend appeared at around time 4.4 s to time 4.5 s due to the aerodynamic impact force in the negative direction during the meeting process. The SME Mining Engineering Handbook said that the aerodynamic buffeting forces are inconsequential and do not need to be considered when designing a rope-guided shaft [20], but the lateral acceleration and lateral velocity show that the aerodynamic buffeting forces should be considered when designing a shaft equipped with rope guides.

As the hoisting speed was proportional to the square of the sum of the ventilation speed, and the lateral aerodynamic force of the lowering conveyance was proportional to the square of the difference between the lowering speed and the ventilation speed. As shown in TABLE 2, the oscillation amplitude of the hoisting conveyance in the south manifested distinctly larger than that of the lowering conveyance in the north.

As shown in Fig. 11, the size of the clearance between the guide sleeve and the guide rope directly affected the lateral oscillation characteristics of the hoisting conveyance. The lateral oscillation amplitude of the hoisting conveyance showed a positive correlation with the clearance. The elastic restoring force of the guide rope was reduced with the increasing clearance, so the lateral oscillation amplitudes of the hoisting conveyances were increased with the clearance.

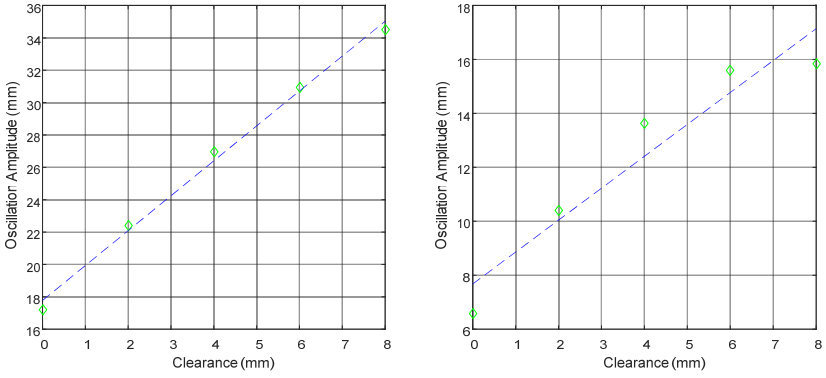

(a) The ascending conveyance (b) The descending conveyance

Fig. 11. The variation of lateral oscillation amplitude of the conveyances with clearances

TABLE 2

Summary of maximum displacement with different clearance

Clearance (mm)		0	2	4	6	8
maximum displacement of southern conveyance hoisting up (mm)	southward	14.05	17.58	20.60	23.28	25.73
	northward	–3.14	–4.84	–6.37	–7.68	–8.76
	oscillation amplitude	17.19	22.42	26.97	30.96	34.49
maximum displacement of northern conveyance lowering down (mm)	southward	1.21	2.13	2.62	2.40	1.09
	northward	–5.39	–8.28	–11.02	–13.18	–14.76
	oscillation amplitude	6.59	10.41	13.63	15.58	15.84

4. Conclusions

With the UDFs loaded by Fluent, this paper investigated the behaviour of rope-guided conveyances with the variation of the clearance between the guide sleeve and the guide rope. Results showed that aerodynamic buffeting forces occurred during the passing process. The lateral oscillation of rope-guided conveyances was greatly affected by the clearance between the guide sleeve and the guide rope. CFD simulation was a powerful tool to investigate the behaviour of rope-guided conveyance for the rope-guided hoisting system design. When designing a shaft equipped with rope guides, it is crucial to take into account the aerodynamic buffeting force that may be present.

Acknowledgements

This work was supported by the Open Fund of Mechanical Industry Key Laboratory of Intelligent Mining and Beneficiation Equipment (No. 2022KLMI03), Anhui University-level Special Project of Anhui University of Science and Technology (No. XCZX2021-01), Open Research Grant of Joint National-Local Engineering Research Centre for Safe and Precise Coal Mining (NO. EC2023015), Huainan City Science and Technology Plan Project (No. 2023A3112), Scientific Research Foundation for High-level Talents of Anhui University of Science and Technology (No. 2022yjrc18), Jiangsu Planned Projects for Postdoctoral Research Funds (No. 2018K165C), and Anhui Provincial Natural Science Foundation (No. 2208085ME128).
We are grateful to the Advanced Analysis and Computation Center of China University of Mining and Technology for the award of CPU hours to accomplish this work.

References

[1] R.S. Hamilton, Rope-guided hoisting for 2000 and beyond-engineering rope guides for deep shafts. In: Proceedings of Mine Hoisting 2000, Fifth International Conference, South African Institute of Mining and Metallurgy Symposium Series S25, South African Institute of Mining and Metallurgy, Johannesburg (2000).

[2] W. Slonina, W. Stühler, Safety problems posed by rope shaft guides. Commission of the European Communities (Mines Safety and Health Commission), Luxembourg (1980).

[3] T.H. Han, K.H. Kim, U.C. Han, K.M. Li, Simulation for motion of platform during truck changing in trucklift slope hoisting system in open pit mines using adams and matlab/Simulink. Arch. Min. Sci. **66** (3), 393-406 (2021). DOI: https://doi.org/10.24425/ams.2021.138596

[4] Y. Wang, W.D. Zhu, Z. Kou, Dynamic Simulation of a Dual-Cable Parallel Winding Hoisting System with Flexible Guides. Int. J. Struct. Stab. Dy. **22** (02), 2250018-2250038 (2022). DOI: https://doi.org/10.1142/S0219455422500183

[5] R. Wu, Z. Zhu, G. Cao, Influence of ventilation on flow-induced vibration of rope-guided conveyance. Journal of Vibroengineering **17** (2), 978-987 (2015).

[6] J. Wang, W.T.T. van Horssen, On resonances and transverse and longitudinal oscillations in a hoisting system due to boundary excitations. Nonlinear Dynam. **111** (6), 5079-5106 (2023). DOI: https://doi.org/10.1007/s11071-022-08052-8

[7] M.E. Greenway, The use of rope guides for deep shafts, in: B. Johansson (Eds.), Hoist & Haul 2015: Proceedings of the International Conference on Hoisting and Haulage. The Society for Mining, Metallurgy and Exploration, Stockholm, Sweden (2015).

[8] K.W. Buchinski, Skip rotation: a collision course or controllable motion. In: 11th CIM Underground Operators Conference, Saskatoon (1993).

[9] G.J. Krige, Guidelines for the design of rope guides, in: Hoist & Haul 2005: Proceedings of the International Conference on Hoisting and Haulage. Australasian Institute of Mining and Metallurgy, Perth (2005).

[10] M. Greenway, B. Jujnovich, S. Grobler, N. Baroni, Behaviour of rope guided conveyances. In: Proceedings of Mine Hoisting 2000, Fifth International Conference, South African Institute of Mining and Metallurgy Symposium Series S25, South African Institute of Mining and Metallurgy, Johannesburg (2000).

[11] Xu, C., Simulation and Computing of Lateral Aerodynamic Force on Hoisted Container with Rope Guide. Mod. Min. **50** (1), 138-142 (2019). [in Chinese]. DOI: https://doi.org/10.3969/j.issn.1674-6082.2019.01.034

[12] S. Quan, T. Li, J. Butty, Investigation on Conveyance Motion Using CFD and Structural Analysis. In: B. Johansson (Eds.), Hoist & Haul 2015: Proceedings of the International Conference on Hoisting and Haulage, The Society for Mining, Metallurgy and Exploration, Stockholm, Sweden (2015).

[13] G.J. Krige, Development of Design Guidelines for Rope Guided Hoisting Report 1: CFD Results. Anglo Technical Division, Johannesburg (2001).

[14] R. Wu, Z. Zhu, G. Cao, Computational fluid dynamics modeling of rope-guided conveyances in two typical kinds of shaft layouts. PLoS One **10** (2), e118268 (2015). DOI: https://doi.org/10.1371/journal.pone.0118268

[15] J.S. Haddad, O. Denyshchenko, D. Kolosov, S. Bartashevskyi, V. Rastsvietaiev, O. Cherniaiev, Reducing Wear of the Mine Ropeways Components Basing Upon the Studies. Arch. Min. Sci. **66** (4), 579-594 (2021). DOI: https://doi.org/10.24425/ams.2021.139598

[16] R. Wu, Z. Zhu, G. Chen, G. Cao, W. Li, Simulation of the lateral oscillation of rope-guided conveyance based on fluid-structure interaction. J. Vibroeng. **16**(3), 1555-1563 (2014).

[17] R.T. Ratan, Surface and Underground Excavations: Methods. Techniques and Equipment (2nd Edition), CRC Press (2013). ISBN 978-0-415-62119-9.

[18] S.S. Rao, Mechanical Vibrations (5th Edition). Prentice Hall (2011). ISBN 978-0-13212-819-3.

[19] J. Janus, Air flow modelling on the geometry reflecting the actual shape of the longwall area and goafs. Arch. Min. Sci. **66** (4), 495-509 (2021). DOI: https://doi.org/10.24425/ams.2021.139593

[20] P. Darling, SME Mining Engineering Handbook (3rd Edition). Society for Mining, Metallurgy, and Exploration, Inc., Littleton (2011). ISBN 978-0-87335-264-2.